An Experimental Model for the Sharp Flat Plate in Rarefied Hypersonic Flow

W. J. McCroskey,* S. M. Bogdonoff,† and J. G. McDougall‡
Princeton University, Princeton, N. J.

Flowfield studies of the shock wave and boundary-layer development on a flat plate are presented for a region that bridges the gap between a classical hypersonic boundary layer downstream and a kinetic flow model at the leading edge. The measurements give a comprehensive picture of the flow pattern in the "merged" or "viscous layer" regime, which exists upstream of the region of validity of hypersonic viscous interaction theory. The results are derived from a combination of several probing and optical techniques and surface pressure measurements. Previous models of slip flow or wedge-like flow were not supported. The shock wave was found to be quite different in thickness and structure from the classical picture of an oblique Rankine-Hugoniot shock, and these effects have not been treated adequately in existing theories. A true scale diagram of the flowfield is given which now makes it possible to evaluate more realistically the theoretical models that have been proposed.

Nomenclature

C = Chapman-Rubesin viscosity constant[15]
h = enthalpy
M = Mach number
p = pressure
$\bar{Q}$ = average heat-transfer rate per unit area to probe
Re = Reynolds number, $\rho_\infty u_\infty x/\mu_\infty$
$\bar{r}$ = recovery factor for probe
St = Stanton number for probe
T = temperature
u = velocity
$\bar{V}$ = rarefaction parameter, $M_\infty(C/Re_x)^{1/2}$
x = longitudinal coordinate
y = normal coordinate
γ = specific heat ratio
Δ = shock wave "maximum slope" thickness
δ^* = displacement thickness
ζ = slip dimension[1]
θ = shock wave angle
λ = mean free path
μ = viscosity
ρ = density
$\bar{\chi}$ = hypersonic viscous interaction parameter, $M_\infty^3(C/Re_x)^{1/2}$

Subscripts

∞ = freestream conditions
o = stagnation conditions
w = conditions at wall of model or probe
aw = adiabatic condition of probe
s = conditions immediately behind shock wave
n = component normal to shock wave
t = component tangent to shock wave

I. Introduction

THE hypersonic flow over a sharp flat plate is a classical problem in the mechanics of viscous fluids which has been studied by many investigators over the past decade. Within the framework of continuum fluid mechanics, the flat plate configuration provides one of the few examples where the ideal potential flow is completely undisturbed, if the leading edge is mathematically sharp. Therefore, it is a particularly appropriate model to examine the effects on the flowfield development due to viscosity, apart from complicating effects of body geometry.

Under conditions of highly rarefied flow, a sharp flat plate generates a wide spectrum of flow regimes. These range from a kinetic theory description of individual molecular encounters at the leading edge, to the continuum picture of a classical boundary layer far downstream. In contrast to the problems involving blunt bodies, the behavior in the intermediate regimes appears to depend upon the freestream Mach number. The present investigation is concerned primarily with that part of the sharp leading edge problem at large Mach numbers which is referred to as the "viscous layer" or "merged layer" regime, sketched in Fig. 1.

It is well known that the development of a viscous boundary layer near the surface of the plate serves to generate a shock wave in the flowfield. The merged layer region is defined as beginning at the first point along the plate where any part of the phenomenon can be described by the equations of continuum fluid mechanics. The downstream limit occurs when a distinct inviscid layer of flow develops between the shock wave and the viscous layer adjacent to the plate. The merged layer regime thus bridges the gap between the kinetic flow region, of which little presently is known, and the "hypersonic viscous interaction" region, which is understood relatively well. In the merged layer regime, surface pressure and heat transfer are less substantially than would be predicted by extrapolation of strong interaction theory to the same point, but the values generally are greater than the free molecule estimates.

Previous Flow Models

The general flow model that has emerged from previous studies consists of the regions indicated in Fig. 1. It is important that the plate be considered mathematically sharp. The basic approach in the past has been to start with strong interaction concepts and to look for changes from these predictions in the merged layer regime. These changes first were attributed to some form of slip phenomena, and, as a result, the upstream limit of the continuum picture often is called the slip flow regime.

On the basis of schlieren, surface pressure, and heat-transfer observations, Nagamatsu, et al.[1,2] have proposed the slip

Presented as Preprint 66-31 at the AIAA 3rd Aerospace Sciences Meeting, New York, January 24–26, 1966; submitted February 2, 1966; revision received May 31, 1966. This study was sponsored by Aerospace Research Laboratories, Office of Aerospace Research, U.S. Air Force, under Contract AF 33(615)-3328 and by the U.S. Air Force Office of Scientific Research, under Contract AF 49(638)-1271.

* Research Associate, Gas Dynamics Laboratory. Student Member AIAA.
† Professor, Head of Gas Dynamics Laboratory. Fellow AIAA.
‡ Assistant in Research, presently with the Boeing Company, Seattle.

flow model shown in Fig. 2a. They say that the shock wave is delayed in forming in the leading edge slip region, and that when the shock wave does form, it is merged with the boundary layer. Furthermore, the shock wave angle does not reach a maximum value until the end of the slip region. Their experimental results showing plateaus of constant pressure and heat transfer are attributed to the shape of the shock wave. Although there is some dissatisfaction with the notion of reverse curvature of the shock wave, the Nagamatsu model is quoted widely in the literature. The conditions required for the model are large Mach number and large Knudsen number (based on the leading edge thickness and λ_∞).

Laurmann[3] has proposed a slightly different slip flow model (Fig. 2b), on the basis of an analysis of the Oseen equations in the hypersonic limit. At the leading edge, the analysis shows perfect slip, i.e., $u_w = u_\infty$, and a displacement thickness behavior that produces coalescing compression waves. The changes that would arise due to the highly nonlinear features of the problem and large viscous dissipation have not been estimated.

Somewhat different ideas on the flow model have emerged from a group of investigators who have followed the order of magnitude arguments of Hayes and Probstein.[4] This approach led Oguchi[5] and a large number of subsequent authors to propose the viscous wedge flow model (Fig. 2c). The shock wave is taken to be straight essentially, with infinitesimal thickness in the merged layer regime, and as a result the pressure is approximately constant. Oguchi found that velocity slip and temperature jump caused significant decreases in heat transfer and pressure. With slip, Oguchi's resultant shock wave has some reverse curvature, although this point generally has not been recognized. Unfortunately, the analysis was done incorrectly§ and therefore the details of the results are open to question.

Two recent theoretical studies have drawn attention to certain specific features of the leading edge problem, although the basic pictures in Fig. 2 are not greatly altered. Pan and Probstein[8] have considered the effects of adding surface slip, shock wave curvature and structure, and normal pressure gradients to the basic viscous wedge flow model of Oguchi.[5] The assumption of local similarity is invoked in the analysis and longitudinal pressure gradients are neglected arbitrarily. Their results for typical examples show heat transfer tending to level off, but both the pressure and the pressure gradients continually increase as the leading edge is approached. Garvine,[7] on the other hand, has concluded that the most crucial element in the problem is the streamwise variation in the flowfield profiles. As a result, the flow in the merged layer regime depends critically on its upstream history, and the governing equations cannot be solved without accurate knowledge of the initial flow conditions at the upstream edge of the continuum regime. This conclusion clearly contradicts the local similarity assumption of Pan and Probstein[8] and indicates the complicated nature of the flowfield structure.

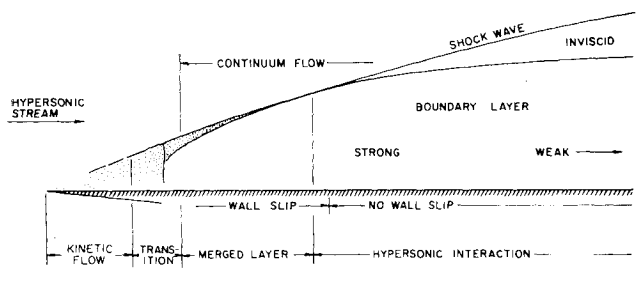

Fig. 1 Schematic flowfield for the sharp leading edge problem.[8]

§ See Aroesty[6] and Garvine,[7] for example.

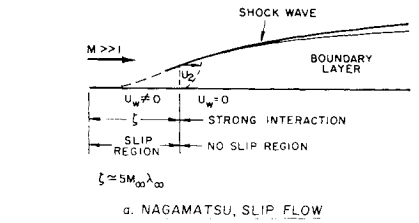

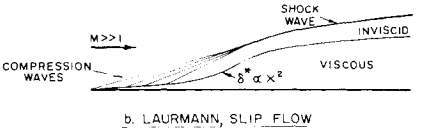

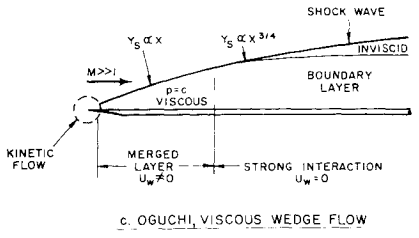

Fig. 2 Flow models proposed by Nagamatsu, et al.,[1,2] Laurmann,[3] and Oguchi.[5]

From the experimental point of view, the primary data in the merged layer regime have been supplied by Nagamatsu et al.,[1,2] Vidal and Wittliff,[9] Chuan and Waiter,[10] Wallace and Burke,[11] and Schaaf et al.[12] The most common measurements have been surface pressure and heat transfer. An assessment of the data available shows considerable disagreement and little correlation, except that the initial departures from strong interaction theory occur at values of the rarefaction parameter $\bar{V} = M_\infty(C/Re_x)^{1/2}$ from about 0.1 to 0.3. Certainly, accurate measurements under these conditions are extremely difficult to obtain, and considerable question exists as to the interpretation of schlieren photographs, corrections to pressure measurements, the significance of nonuniform flow, and the effects of flow angularity. At best, however, these experiments have lacked sufficient detail to construct an accurate model of the flowfield, or to examine closely the theoretical models.

II. Present Investigation

The current situation regarding the sharp leading edge problem is one of several conflicting viewpoints. Various theoretical studies have proposed a number of models to which analyses have been applied, and previous experiments have failed to answer a number of fundamental questions about the theories. An accurate physical model in the leading edge region is missing. The present experiments were designed primarily to supply this kind of information about the merged layer region and the transition to the strong interaction regime.

The experimental program was planned largely around the need for detailed flowfield surveys, and considerable emphasis was placed upon obtaining duplicate or redundant measurements whenever possible. Three different probe techniques were employed, including one probe on a free molecular scale, and both schlieren and glow discharge methods were used for flow visualization. The different techniques were sensitive to momentum flux, mass flow, density, and density gradients. Surface pressure data were obtained to complement the flowfield studies, and heat-transfer tests are planned for the near future. Some preliminary results of the present investigation have been reported by Bogdonoff.[13]

Facility and Models

The experiments were conducted under steadystate conditions in the Gas Dynamics Laboratory Hypersonic Nitrogen

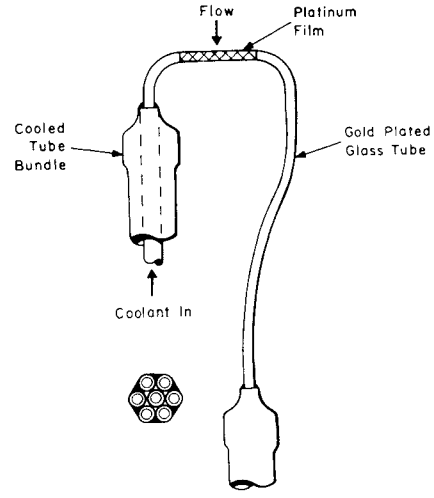

Fig. 3 Tip of the heat flux probe; diameter of the sensor is 0.006 in.

Tunnel N-3. A full description of this facility has been given by Vas and Koppenwallner.[14] Tunnel N-3 is a continuous facility in which the nitrogen test gas is heated by a graphite resistance element in the stagnation chamber. The flow expands into a 6-in.-diam test section, which has a useable core of about 2.5 in. in diameter. The nozzle flow is frozen vibrationally and $\gamma = 1.4$ in the test secton.[14]

The nominal freestream test conditions were the following: $T_o = 3600°$R; $p_o = 2000$–5000 psi; $M_\infty = 23.3$–25.6; and $Re_\infty/\text{in.} = 7500$–$15000$. For these conditions the freestream mean free path varied from about 0.0025 to 0.0045 in., and the merged layer region covered an area on the plate on the order of 2 in. long by $\frac{1}{2}$ in. thick. The Chapman-Rubesin constant was evaluated according to the definition of Cheng, et al.[15] and is about 0.72 for the present data. The value based on μ_∞ and T_∞ would be approximately 0.85.

The theoretical "sharp" leading edge was closely approximated by two test models with leading edge thicknesses about $\frac{1}{3}$ to $\frac{1}{5}$ times λ_∞. The models were sting-mounted in alignment with the tunnel centerline and completely spanned the test core. The wedge angles on the bottom surfaces were 20° and 30°. Internal cooling maintained the surface temperature at about 530°R. Surface pressures were measured using conventional static pressure orifices and individually calibrated variable reluctance transducers. Orifice corrections on the order of 15% were applied to the pressure data, based on the work of Potter et al.[16]

Flowfield Instrumentation

The use of a continuous wind tunnel permitted detailed probing of the flowfield. Small pitot pressure probes were made from flattened tubes that had outside dimensions of 0.011 by 0.12 in. Surveys also were made with a new type of mass flow probe, which consists of a platinum plated internally cooled glass tube with an outside diameter of 0.006 in. This instrument, which is referred to by the manufacturer¶ as the "heat flux probe," was operated as a constant-temperature hot wire anemometer with a large negative overheat ratio $(T_w - T_{aw})/T_{aw}$. The tip of the heat flux probe, including the glass tube, is shown in Fig. 3. Radiation cooled hot wire probes, consisting of 0.0005-in.-diam tungsten wires, were used to supplement the data taken with the heat flux probe. As these fine wires were much smaller than a mean free path, they also served to substantiate the data obtained with the larger probes.

Schlieren photographs were taken with a conventional single pass system. Because of the low level of density gradients encountered in the present investigation, a clearly discernible shock wave shape could be obtained for the highest Reynolds number case only. A typical photograph is shown in Fig. 4. However, a distinct boundary at the outer edge of the disturbed flowfield could be observed for all test conditions when the nitrogen glow discharge technique was used. The "glow" was obtained by placing an air-cooled cathode far enough above the plate surface that shock waves from the two bodies did not interact in the region of interest. A potential of about 800 v d.c. was placed between the cathode and the tunnel walls. The resulting glow was intense enough to permit a simple time exposure photograph, such as the one shown in Fig. 4, to be taken from outside the tunnel.

¶ Thermo-Systems Inc., Minneapolis.

Data Evaluation

The quantitative interpretation of the probe data is complicated by the fact that none of the readings correspond directly to the primary quantities of interest, such as velocity, density, static pressure, etc. However, most of the measurements were in regions of hypersonic flow, so that the response of the pitot probes was proportional to the local momentum flux ρu^2. The probes were calibrated individually for viscous corrections that ranged from about -2 to $+5\%$.

The use of the heat flux probe at the high stagnation temperatures precluded measuring or inferring T_{aw} directly, as is normally done in hot wire anemometry. The supplementary information was supplied by the equilibrium temperature of the radiating hot wire. The basic idea of the scheme employed is that both probes respond to complicated combinations of mass flow and total temperature, but the response is different in each case so that meaningful data can be extracted from the combined measurements. The actual process of analyzing the data further was facilitated by the use of the following hypersonic approximation for the convective heat transfer to a highly cooled cylinder:

$$\bar{Q} = \rho u\, St\, C_p(\bar{r}T_o - T_w)$$

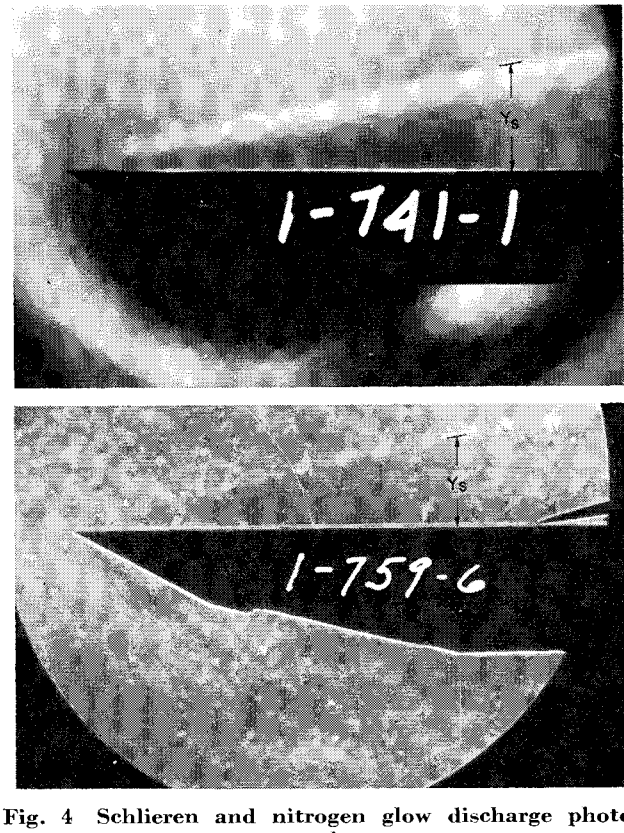

Fig. 4 Schlieren and nitrogen glow discharge photographs.

$$\bar{Q} = \rho u^3 \bar{r}\, St \left[\frac{1}{2} + \frac{1}{(\gamma - 1)M^2} - \frac{C_p T_w}{u^2}\right]$$

$$\bar{Q} \simeq \rho u^3 (\bar{r} St/2)$$

(Here the subscript w refers to the wall of the probe.) Furthermore, the test conditions were such that the Stanton number for the heat flux probe was only weakly dependent upon the local Reynolds number.

Density was calculated from the combined readings of the heat flux probe, the radiating hot wire, and the pitot probe. The details of the computational technique, which is rather lengthy, are given in Ref. 17. The measurements of density are considered accurate to within $\pm 10\%$ in the strong interaction region and $\pm 20\%$ at the upstream limit of $x = 0.1$ in. It is noteworthy that in most cases the integrated measurements of mass flux across the flowfield checked with the freestream values to within 5%.

III. Discussion of the Flow Model

Onset of Merging

At the downstream limit of the merged layer regime, the shock wave and boundary layer begin to be separated by a region of essentially inviscid but rotational flow. This does not occur abruptly, but can be detected by the probe survey profiles as well as on schlieren photographs. The response of the heat flux probe at several axial stations is shown in Fig. 5, where the differences in merged layer and strong interaction profiles are apparent. Profiles taken with small pitot tubes are qualitatively the same. For the present tests, the inviscid layer becomes indistinguishable at values of $\bar{V} = M_\infty (C/Re_x)^{1/2}$ of about 0.15, and the region $0.15 < \bar{V} < 0.20$ is considered the boundary between the strong interaction and fully merged regimes. This result agrees with estimates of Talbot[18] and Dewey,[19] based on surface measurements, for the upstream limit of hypersonic viscous interaction theory.

Effects of Merging

The most striking effect that occurs in the flowfield near the leading edge is the disappearance of the classical picture of a Rankine-Hugoniot shock wave. A close examination of the direct probe surveys in Fig. 5 and the density profiles in Fig. 6 gives a clear picture of the change in the structure of the merged region as the leading edge is approached. For the particular conditions of this test, the survey at 3 in. is in the strong interaction region, $x = 2$ in. is approximately the strong interaction limit, and the surveys at 1 and at

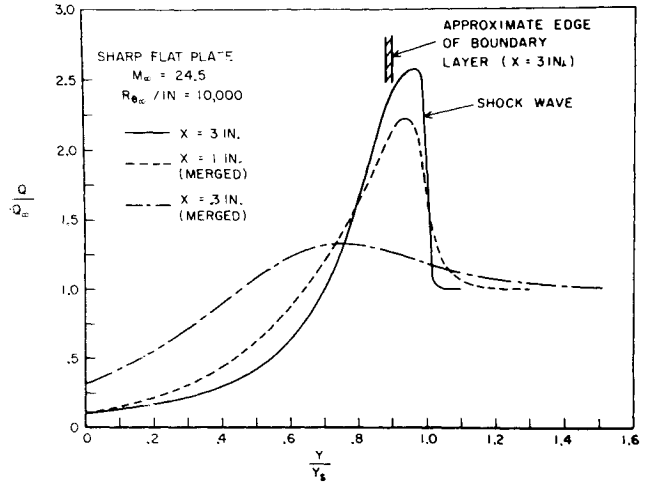

Fig. 5 Flowfield profiles with the heat flux probe. $Q \propto \rho u (\bar{r} T_0 - T_w)$.

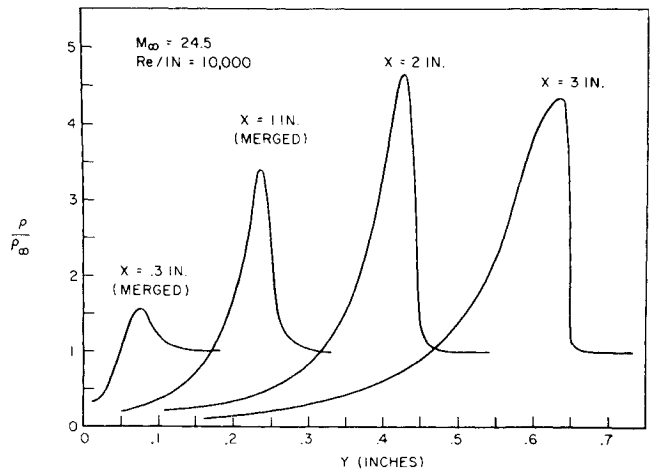

Fig. 6 Density profiles at the intermediate freestream conditions.

0.3 in. are deep in the merged region. It is quite clear that as soon as the viscous region merges with the shock wave, large changes occur, both in the level of the peak density and the thickness of the shock wave. The outer boundary of the disturbed flowfield is no longer a shock wave in the usual sense, but for lack of a better definition, this boundary still will be referred to as a shock wave. The sketches in Fig. 7 show the definitions of the thickness (Δ_s = maximum slope thickness) and the position y_s of the shock wave used in the present paper.**

The schlieren, glow, and probe data can be combined to give the shock wave shape and location, shown in Fig. 8 for two freestream conditions. Each symbol represents the average of many data points. The good agreement of the several techniques lends substantial support to the use of these data. However, the density gradients decrease markedly near the leading edge, as indicated in the subsequent discussion, and the sensitivity of the schlieren technique decreases correspondingly. As a result, the other techniques are much more valuable in this region.

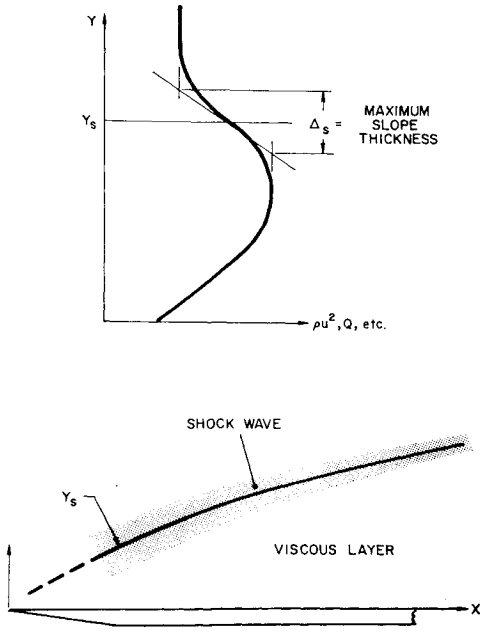

Fig. 7 Shock wave nomenclature.

** In the case of the nitrogen glow discharge technique, the position of the shock wave was taken as the outer boundary of the region of maximum intensity, as indicated in Fig. 4.

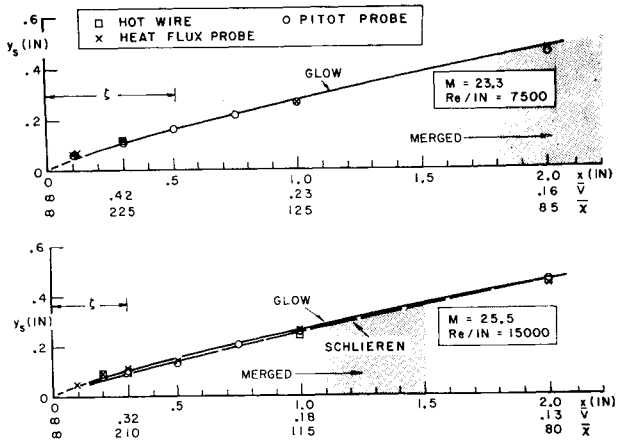

Fig. 8 Combined shock wave shapes from probes and optical techniques. ζ is the Nagamatsu slip dimension.[2]

One of the most interesting features of the data in Fig. 8 is that the shock shape clearly is convex everywhere, with no indication of the reverse curvature of the Nagamatsu slip flow model.[1,2] The smooth continuous behavior of the shock wave extends all the way from the strong interaction region to the kinetic flow region near the leading edge. On each plot, the size of the Nagamatsu "slip distance" ζ is shown, but insofar as shock shape is concerned, this dimension does not appear to be relevant to the present experiments.

A plot of these same data on logarithmic scales (Fig. 9) shows that the present measurements closely approximate the $\frac{3}{4}$ power law strong interaction theory of Cheng et al.[15] Shock shape data from other cold wall investigations,[11,20] and Chuan and Waiter's adiabatic wall results[10] also are shown. For the Chuan and Waiter data y_p and y_s denote the location of the peak pitot pressure and the center of the maximum slope thickness, respectively. The differences between the Chuan and Waiter data and the other measurements probably can be attributed to the differences in the wall temperature ratio. It is difficult to estimate the curvature from these data, but the trend seems to be that the curvature is somewhat less than predicted by strong interaction theory. At the same time, the approximate position of the shock wave can be estimated fairly well using strong interaction theory.

Although the shock wave shape is relatively insensitive to the changes in the flowfield structure, the ratio of shock wave thickness to shock layer thickness provides a dramatic demonstration of the effects of merging. This ratio is plotted in Fig. 10 vs the rarefaction parameter $\bar{V}$, where Δ_s and y_s are the quantities that were defined previously in Fig. 7. A sudden increase in the thickness ratio occurs at a

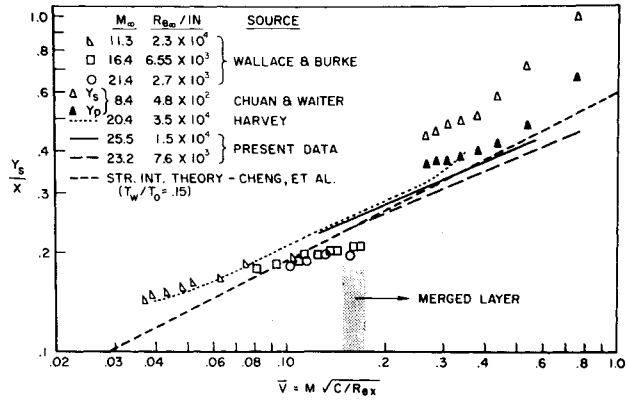

Fig. 9 Correlated shock wave shapes in air and nitrogen. Cold wall data, except Chuan and Waiter.[10]

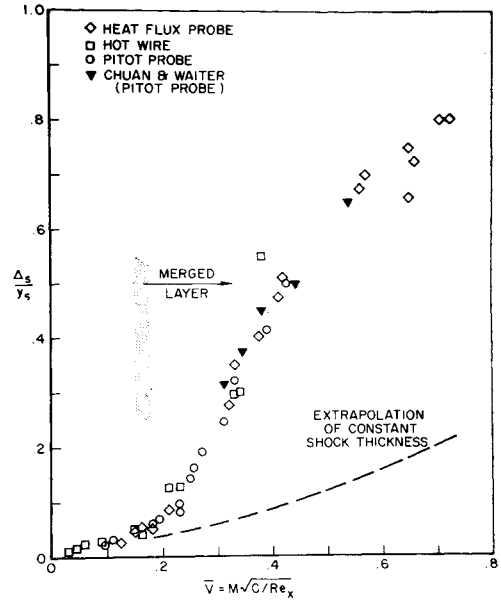

Fig. 10 Ratio of shock wave thickness to shock layer thickness.

value of $\bar{V}$ of about 0.19 to 0.20, following the onset of merging. The results for larger values of $\bar{V}$ are particularly interesting, as Δ_s/y_s is zero in the Oguchi model[5] and small in the Pan and Probstein theory.[8] In fact, Pan and Probstein estimate the shock thickness effects will only be important for $Re_x/M_\infty \geq 40$–45, and this would correspond to a point in the present experiments where the actual shock thickness seems to be well over half the shock layer thickness. If the shock wave thickness were constant, as implicitly assumed in all previous order of magnitude estimates, then Δ_s/y_s would follow the qualitative trend indicated in the figure. It should be emphasized that the same results were obtained with all three probe techniques, one of which was free molecular. This correlation covers tests in both helium and nitrogen at Princeton at Mach numbers of 16 and 24 and is supported by the data of Chuan and Waiter[10] at a Mach number of eight.

The strength of the shock wave also depends crucially upon whether the shock wave and viscous layer are merged. The nature of the flowfield is such that peak values of density, mass flow, pitot pressure, etc. are associated with the downstream edge of the shock wave or outer transition boundary. The probe data were combined to give the maximum value of density for each survey, shown in Fig. 11 as a function of $\bar{V}$. Representative uncertainties are indicated in this figure. Also shown is a band representing the theoretical Rankine-Hugoniot density ratios, i.e., ρ_s/ρ_∞ for straight, oblique shock waves with no shear stress or heat conduction at the rear surface and with the measured shock angles (allowing tolerances of $\pm 1°$). The Rankine-Hugoniot density ratio increases somewhat as the leading is approached, because the shock angle increases. However, the measured density ratios in the merged region fall far below the Rankine-Hugoniot values, indicating that the structure of the shock wave is altered drastically by the viscous layer. It seems unlikely that curvature alone could account for the observed behavior.

The density measurements reveal striking departures from the classical picture of a Rankine-Hugoniot shock wave that generally has been assumed to apply over most of the merged layer regime. However, most of the theories available do not even consider this effect, and the Pan and Probstein theory[8] falls far short of predicting the observed behavior. For example, at $\bar{V} = 0.25$ for the present freestream conditions, the actual value of ρ_s/ρ_∞ would be approximately 50% of the Rankine-Hugoniot value, whereas Pan and Probstein would predict a reduction of less than 5%. On the other

hand, the measurements do not reveal any significant effect of the merging upon the velocity ratio u_s/u_∞.

Surface Pressure Distribution

It has been well established by previous experiments[1,2,9-12] that the hypersonic viscous interaction theory is not valid sufficiently close to the leading edge. Talbot[18] has proposed the parameter $\bar{V} = M_\infty(C/Re_x)^{1/2}$ to correlate the initial departures from viscous interaction theory, and this departure seems to occur at $0.1 < \bar{V} < 0.3$ for most surface data available. Such behavior is apparent for the present data (plotted in Fig. 12), where the coordinates are such that strong interaction theory predicts a horizontal straight line. Also shown on the plot are surface pressure data of Vidal et al.,[9,21] which include orifice corrections. The present measurements show $p_w \propto \bar{\chi}$ downstream of $\bar{V} \simeq 0.15$, but a change in this trend is apparent in the merged region. No plateaus of constant pressure were found in the present experiments. The peak pressure apparently occurs upstream of $\bar{V} = 0.5$.

The surface pressure distribution is particularly interesting in the light of the previous discussions about the density ratio across the shock wave. The common factor in both the flowfield studies and the surface pressure measurements is the significant change that occurs when the boundary layer merges into the shock wave. It would appear that a large part of the behavior of the surface pressure is caused by the change in shock structure which accompanies the merging. Some basis for this speculation is provided by the following argument.

The Rankine-Hugoniot relationships describing the changes that occur across an oblique shock wave are derived from the following basic conservation laws:

Continuity

$$\rho_\infty u_{n\infty} = \rho_s u_{ns} \tag{1}$$

Normal Momentum

$$p_\infty + \rho_\infty u_{ns}^2 = p_s + \rho_s u_{n\infty}^2 \tag{2}$$

Tangential Momentum

$$u_{t\infty} = u_{ts} \tag{3}$$

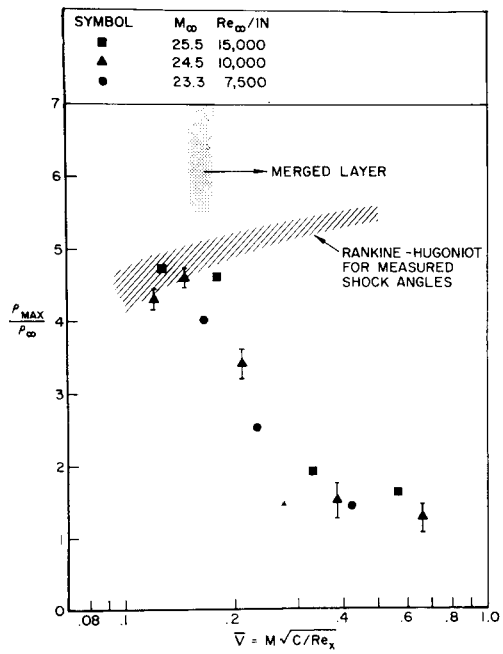

Fig. 11 Density ratio across the shock wave in the merged layer regime.

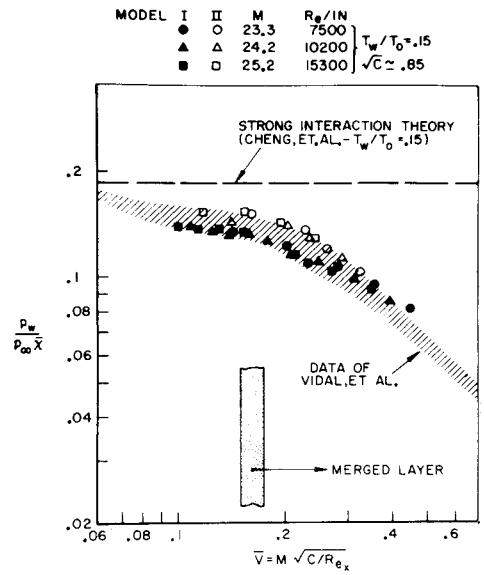

Fig. 12 Correlation of surface pressure. Data corrected for orifice effect.

Energy

$$h_\infty + u_\infty^2/2 = h_s + u_s^2/2 \tag{4}$$

For the case of a thick, curved shock with finite shear stress and heat conduction downstream, the tangential momentum and energy Eqs. (3) and (4) obviously are not valid. Also, normal shear stress and curvature terms should be added to the normal momentum equation. However, the work of Liepmann et al.[22] would seem to indicate that the normal shear stress is of secondary importance, and the radius of curvature is on the order of 100 Δ_s for the present measurements. Therefore, as a first approximation, the relationship between pressure and density can be estimated by using a standard combination of the continuity and normal momentum equations, i.e.,

$$p_s - p_\infty = \rho_\infty u_{n\infty}^2[1 - (\rho_\infty/\rho_s)] \tag{5}$$

or

$$(p_s - p_\infty)/\rho_\infty u_\infty^2 = [1 - (\rho_\infty/\rho_s)] \sin^2\theta_s \tag{6}$$

The main conclusion to be drawn from this argument is that changes in the shock wave structure which effect the density ratio ρ_s/ρ_∞ likewise should effect the pressure ratio p_s/p_∞. The experimental values of ρ_s/ρ_∞ and the shock wave angles have been inserted into Eq. (6) to provide an estimate of the pressure rise across the shock wave. The results are shown in Fig. 13 as a function of $\bar{V}$. The theoretical pressure behind a Rankine-Hugoniot shock wave is indicated, based on measured values of θ_s. Also shown on the plot are the surface pressure data from Fig. 12.

In the strong interaction regime, $M_\infty(C/Re_x)^{1/2} < 0.15$, the pressure given by Eq. (6) approximately is equal to the Rankine-Hugoniot value. Both values are substantially greater than the measured pressure on the surface. This is partially caused by the streamline curvature in the flowfield. As the leading edge is approached, the surface pressure and the estimated pressure behind the shock tend to level off, while the theoretical shock pressure increases to more than three times the surface value. It seems unlikely that the observed behavior solely could be attributed to curvature; rather, the shock wave structure seems to be a dominant mechanism in determining the surface pressure. It should be emphasized that Fig. 13 is not offered as a presentation of quantitative data, but as an attempt to extract the maximum amount of qualitative information from the present experiments.

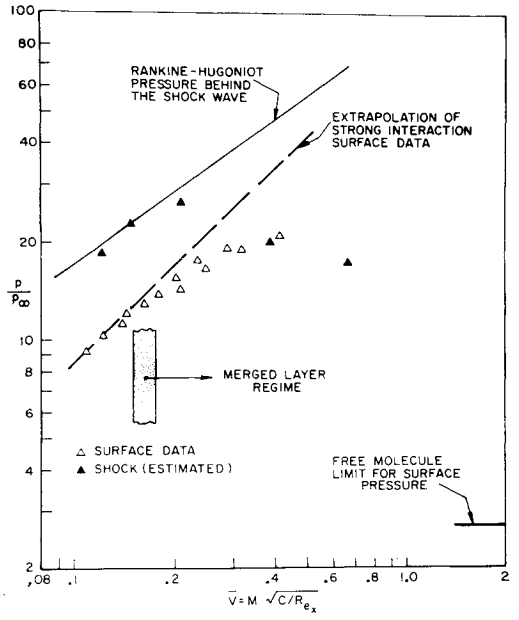

Fig. 13 Comparison of surface pressure with estimated pressure behind the shock wave. M = 24.5, Re/in. = 10,000.

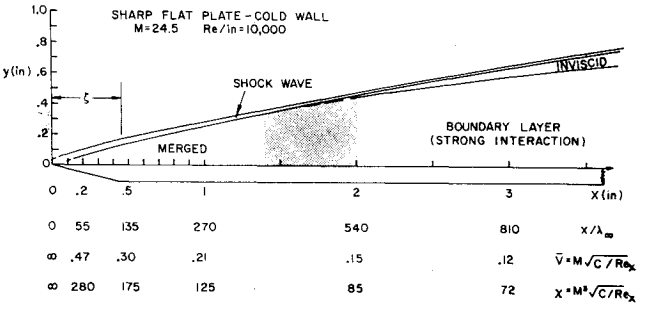

Fig. 14 True scale model of the flowfield. Shock wave drawn according to maximum slope thickness.

True Scale Flowfield

With the position and thickness dimensions from the probe studies and the details of the point where the merging occurs, a true scale accurate physical model of the flowfield can be constructed. This combined information is shown in Fig. 14. The horizontal scales include x/λ_∞, the rarefaction parameter $\bar{V}$, the hypersonic interaction parameter $\bar{\chi}$, as well as the physical dimensions, to provide a basis for comparison with the theoretical models. The shock wave is drawn on the diagram according to the "maximum slope" thickness defined in Fig. 7. The shock wave thickness in the strong interaction region is about five freestream mean free paths. The thickness based on other definitions, such as a discernible change from the freestream, would be considerably larger than the maximum slope thickness, so that the shock wave actually extends well beyond the solid lines that are drawn. In any case, the shock wave is definitely not thin compared to the viscous layer thickness, except in the strong interaction region.

Upstream of $\bar{V}$ approximately 0.17 to 0.19, the flow is considered to be fully merged and the strong interaction model no longer applies. The dimension proposed by Nagamatsu et al.[1] for slip effects is more than 100 mean free paths. The present results show that the shock structure is changing in this region, but there is no indication of the reverse curvature and delay in forming of the flowfield that are featured in the Nagamatsu[1] and Laurmann[3] models. The shock is everywhere convex.

The kinetic region was too small to explore in detail, but under the conditions studied, the shock wave can be considered as coming from or slightly ahead of the leading edge. This interesting behavior contradicts the commonly assumed picture of a region of free molecule flow at the leading edge. Likewise, the extrapolated surface pressure distribution would seem to be far above the free molecule limit (see Fig. 13). It may be mentioned that similar results were obtained in Chuan and Waiter's experiments[10] and in Bird's recent computer experiments.[23]

IV. Concluding Remarks

The combined information from the various experimental techniques gives a comprehensive picture of the shock wave and boundary-layer development on a sharp flat plate. With this information it has now become possible to evaluate more realistically the theoretical models that have been proposed. No indication of the Nagamatsu slip flow model was observed, even though the slip distance extended a considerable length along the plate. At the same time the thin, straight Rankine-Hugoniot shock of the Oguchi viscous wedge model was not supported by the present study because the shock wave is neither thin nor straight nor Rankine-Hugoniot in the merged layer region. Furthermore, the structure of the shock wave is so different from the classical Rankine-Hugoniot picture that Pan and Probstein's attempt to extrapolate their flow model and analysis to within five to ten mean free paths of the leading edge does not seem to be justified.

To summarize the results of the present investigation, information has been presented which now can be used to evaluate theoretical calculations of shock wave thickness, shock layer thickness, and density behind the shock. The strong interaction model was found to have a definite upstream limit that occurs when the boundary layer merges into the shock wave. This merging occurs at $M_\infty(C/Re_x)^{1/2} \simeq 0.15 - 0.20$, and $\bar{\chi}$ is not the relevant parameter upstream of the strong interaction region. Similar results are apparent in previous data over a wide range of Mach numbers.

The shock wave is slightly curved, although this effect does not seem to be as important as the thickness and structure of the shock. The merging of the shock wave and boundary layer is accompanied by large reductions in the maximum values of density. This phenomenon indicates that the structure of the shock wave plays a dominant role in establishing the surface pressure distribution that is observed in the merged layer regime. The shock structure effects are the main points in which the present flow model differs from previous proposals and are the most important results of the investigation.

References

[1] Nagamatsu, H. T. and Sheer, R. E., Jr., "Hypersonic shock wave boundary layer interaction with leading edge slip," ARS J. **30**, 454–462 (1960).

[2] Nagamatsu, H. T., Weil, J. A., and Sheer, R. E., Jr., "Heat transfer to a flat plate in high temperature rarefied ultrahigh Mach number flow," ARS J. **32**, 533–541 (1962).

[3] Laurmann, J. A., "Structure of the boundary layer at the leading edge of a flat plate in hypersonic slip flow," AIAA J. **2**, 1655–1657 (1964).

[4] Hayes, W. D. and Probstein, R. F., *Hypersonic Flow Theory* (Academic Press Inc., New York, 1959), Chap. X.

[5] Oguchi, H., "Leading edge slip effects in rarefied hypersonic flow," *Rarefied Gas Dynamics*, edited by J. A. Laurmann (Academic Press Inc., New York, 1963), Suppl. 2, Vol. II, p. 181.

[6] Aroesty, J., "Slip flow and hypersonic boundary layers," AIAA J. **2**, 189–190 (1964).

[7] Garvine, R., "On hypersonic viscous flow near a sharp leading edge," Princeton Univ., Dept. of Aerospace and Mechanical Sciences Rept. 755 (1965).

[8] Pan, Y. S. and Probstein, R. F., "Rarefied flow transition at a leading edge," Massachusetts Institute of Technology Fluid Mechanics Lab. Rept. 64–8 (1964).

[9] Vidal, R. J. and Wittliff, C. E., "Hypersonic low density studies of blunt and slender bodies," *Rarefied Gas Dynamics*, edited by J. A. Laurmann (Academic Press Inc., New York, 1963), Suppl. 2, Vol. II, p. 343.

[10] Chuan, R. L. and Waiter, S. A., "Experimental study of hypersonic rarefied flow near the leading edge of a thin flat plate," *Rarefied Gas Dynamics*, edited by J. A. Laurmann (Academic Press Inc., New York, 1963), Suppl. 2, Vol. II, p. 328.

[11] Wallace, J. E. and Burke, A. F., "Skin friction, heat transfer and pressure distributions over a flat plate and highly swept delta wings with sharp and blunt leading edges at angles of attack in hypersonic flow," Aeronautical Systems Div., ASD-TDR-63-772 (1963); also, J. H. De Leeuw (ed.), *Rarefied Gas Dynamics* (Academic Press Inc., New York, 1965), Suppl. 3, Vol. I, p. 487.

[12] Schaaf, S. A., Hurlburt, F. C., Talbot, L., and Aroesty, J., "Viscous interaction experiments at low Reynolds numbers," ARS J. **29**, 527–528 (1959).

[13] Bogdonoff, S. M., "The sharp flat plate in hypersonic flow—a review and preview," *Proceedings of Symposium on Advanced Problems and Methods in Fluid Mechanics* (Jurata, Poland), to be published.

[14] Vas, I. E. and Koppenwallner, G., "The Princeton University high pressure hypersonic nitrogen tunnel N-3," Princeton Univ., Dept. of Aerospace and Mechanical Sciences Rept. 690 (1964).

[15] Cheng, H. K., Hall, J. G., Golian, T. C., and Hertzberg, A., "Boundary layer displacement and leading edge bluntness effects at high temperature hypersonic flow," J. Aerospace Sci. **28**, 353–360 (1961).

[16] Potter, J. L., Kinslow, M., and Boylan, D. E., "An influence of the orifice on measured pressures in rarefied flow," *Rarefied Gas Dynamics*, edited by J. H. deLeeuw (Academic Press Inc., New York, 1966), Suppl. 3, Vol. II, p. 175.

[17] McCroskey, W. J., "An experimental model for the sharp leading edge problem in rarefied hypersonic flow," Aerospace Research Laboratories Rept. ARL 66-0101 (1966).

[18] Talbot, L., "Criterion for slip near the leading edge of a flat plate in hypersonic flow," AIAA J. **1**, 1169–1171 (1963).

[19] Dewey, C. F., Jr., "Bluntness and viscous interaction effects on slender bodies at hypersonic speeds," AIAA Paper 65–43 (1965).

[20] Harvey, W. D., "Effects of leading edge bluntness on pressure and heat transfer measurements over a flat plate at a Mach number of 20," NASA TN-D-2846 (1965).

[21] Vidal, R. J. and Bartz, J. A., "Experimental studies of low-density effects in hypersonic wedge flows," *Rarefied Gas Dynamics*, edited by J. H. deLeeuw (Academic Press Inc., New York, 1965), Suppl. 3, Vol. I, p. 467.

[22] Liepmann, H. W., Narasimha, R., and Chahine, M. T., "Structure of a plane shock wave," Phys. Fluids **5**, 1313–1318 (1962).

[23] Bird, G. A., "Aerodynamic properties of some simple bodies in the hypersonic transition regime," AIAA J. **4**, 55–60 (1966)